Heliyon 10 (2024) e37028

Contents lists available at ScienceDirect

Heliyon

journal homepage: www.cell.com/heliyon

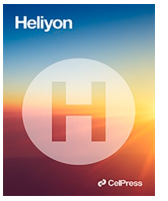

Research article

Identification and functional characterization of differentially expressed circRNAs in high glucose treated endothelial cells: Construction of circRNA-miRNA-mRNA network

Hao Lin [1], Tongqing Yao [1], Haoran Ding, Jiapeng Chu, Deqiang Yuan, Fan Ping, Fei Chen [*], Xuebo Liu [**]

Department of Cardiology, Tongji Hospital, School of Medicine, Tongji University, 200092, Shanghai, China

ARTICLE INFO

Keywords:
RNA-seq
Microarray
circRNAs
ceRNAs network
Endothelial cells dysfunction
High glucose

ABSTRACT

Background: Endothelial dysfunction is a complication of diabetes mellitus (DM), characterized by impaired endothelial function in both microvessels and macrovessels, closely linked to atherosclerosis (AS). Endothelial dysfunction, characterized by impaired endothelial cell (EC) function, is a pivotal factor in AS and DM. Circular RNAs (circRNAs) are endogenous non-coding RNAs that can act as competing endogenous RNAs (ceRNAs) and regulate gene expression. However, the role of circRNAs in ECs dysfunction and AS under high glucose (HG) condition remains elusive.
Methods: We performed high-throughput sequencing to identify differentially expressed (DE) circRNAs in human umbilical vein endothelial cells (HUVEC) exposed to HG, one risk factors of endothelial dysfunction and AS. We then validated eight candidate circRNAs by qRT-PCR and functional analysis, directing our attention to hsa_circ_0122319. Moreover, microarray analysis identified the differential expression profiles of miRNAs and mRNAs regulated by hsa_circ_0122319. Subsequently, the construction of the ceRNAs network employed bioinformatic analysis and Cytoscape software. Furthermore, the role of the PI3K-Akt signaling pathway in regulating ceRNAs was evaluated.
Results: We detected 917 DE circRNAs in HG treated HUVEC. The parental genes of these circRNAs were enriched in cell cycle, cellular senescence and endocytosis related pathways. The differential expression of hsa_circ_0122319 was confirmed to be most obvious at the cellular level and in clinical samples by qPCR experiments. After overexpression of hsa_circ_0122319, 49 DE miRNAs and 459 DE mRNAs were identified using microarray analysis. Subsequently, a ceRNAs network was constructed, comprising hsa_circ_0122319, 8 miRNAs, and 41 mRNAs.
Conclusion: In summary, our study delves into the role of circRNAs in endothelial dysfunction associated with DM and AS. Through high-throughput sequencing and validation, we identified hsa_circ_0122319 as a pivotal regulator of ECs function under HG conditions. It also showed that hsa_circ_0123319 has the potential to serve as a biomarker for DM and its vascular complications, and provides new evidence for future exploration of the intricate molecular mechanisms of endothelial dysfunction in the progression of DM and AS.

* Corresponding author.
** Corresponding author.
E-mail addresses: riverapt@126.com (F. Chen), liuxuebo70@hotmail.com (X. Liu).
[1] These authors contributed equally to this work.

https://doi.org/10.1016/j.heliyon.2024.e37028
Received 10 May 2024; Received in revised form 31 July 2024; Accepted 26 August 2024
Available online 28 August 2024

1. Introduction

Diabetes mellitus (DM) is a chronic metabolic disorder that affects millions of people worldwide. It is characterized by prolonged elevation of blood glucose concentration (hyperglycemia) due to impaired insulin function, which can result from insufficient insulin secretion, insulin resistance, or reduced tissue sensitivity to insulin [1]. One of the complications of DM is endothelial dysfunction, characterized by impaired function of both microvascular and macrovascular endothelium, closely associated with the development of atherosclerosis (AS) and considered a major cause of mortality in DM patients [2]. In numerous studies, aberrant endothelial cells (ECs) injury has been recognized as a critical pathological feature in the progression of AS [3]. To unravel the elusive molecular mechanisms driving ECs dysfunction in DM-associated AS and identify novel therapeutic and preventive targets, a comprehensive investigation of ECs damage is imperative.

Endothelial dysfunction is a key pathological condition characterized by impaired ECs function and plays a crucial role in the development and progression of various cardiovascular diseases. In particular, high glucose (HG) levels have been implicated in the initiation and exacerbation of endothelial dysfunction [4,5]. Studies have shown that prolonged exposure to HG concentrations can lead to oxidative stress, inflammation, and impaired nitric oxide bioavailability, all of which contribute to endothelial dysfunction [6,7]. Therefore, it is crucial to gain a deeper understanding of the specific molecular mechanisms that HG how to regulate endothelial function and the contribution in AS progression.

CircRNAs was first discovered in RNA viruses in 1976, which is a special class of endogenous non-coding RNAs (ncRNAs) with a length that exceeds 200 nucleotides [8]. CircRNAs is widely participated in the physiological and pathological processes by epigenetic, transcription and post-transcriptional regulation [9]. And compared with linear RNAs, circRNAs have characteristic stable structure of covalently closed loops, which strongly indicate that circRNAs could serve as potential biomarkers for multiple disease [10]. In addition, ceRNAs network hypothesis was proposed by Salmena and colleagues [11]. Based on this hypothesis, several circRNAs are considered play crucial role in the regulation mRNA expression by competitive binding miRNA response elements [12]. For example, previous study comprehensive analysis circRNAs expression pattern and ceRNAs network in the pathogenesis of AS in rabbits [13]. In addition, abnormal upregulation of circCHFR in the ox-LDL-induced vascular smooth muscle cell (VSMCs) promotes the proliferation and migration of VSMCs by sponging miR-370, leading to vascular remodeling and the development of AS [14]. Simultaneously, construction of circRNA-linked ceRNAs networks has been performed both in cancer [15] and CVD [13]. However, there is no study on the regulation of endothelial function and the progression of AS based on the competing endogenous RNAs (ceRNAs) network crosstalk under the condition of HG intervention.

For present study, therefore, we employed comprehensive transcriptomic analyses and bioinformatics approaches to identify and functionally characterize differentially expressed (DE) circRNAs in HG-treated ECs. Additionally, we constructed a circRNA-miRNA-mRNA network to explore the potential interactions and regulatory pathways underlying the observed phenotypes. Understanding the dysregulated circRNA-mediated regulatory networks in HG-treated ECs will contribute to the development of novel diagnostic markers and therapeutic strategies to mitigate the complication of endothelial dysfunction in diabetes.

2. Method

2.1. Cell culture, treatment and transfection

The immortalized human endothelial cell (HUVEC) line EAhy926 were purchased from the Chinese Academy of Science and cultured in Dulbecco's Modified Eagle Medium (DMEM, low glucose, 5.5 mmol/L, Hyclone) supplemented with 5 % FBS (Gibco), 3 % penicillin/streptomycin (Gibco). And cells were maintained at 37 °C humidified incubators at 5 % CO2. D-glucose was purchased from sigma (Lot#SLBC6575V). Based on the pre-experiment on the expression levels of SASP and senescence markers in HUVEC after different concentrations of glucose treatment, we chose 30 mmol/L glucose treatment as the HG group. And 30 mmol/L mannitol-treated group was used as osmotic control (Fig. S1).

The two groups of HUVEC included cells transfected with GFP lentiviral vectors for circRNAs over-expression constructs according to the manufacturer's instructions, cells treated with empty GFP lentiviral vectors and non-transfected cells, which all vectors were synthesized from Hanheng biotech company (Shanghai, China).

2.2. RNA extraction and quantification

Extraction of total RNA using the TRIZOL reagent (Invitrogen, CA, United States). And the total RNA was reverse transcribed using PrimeScript™ RT Master Mix (RR036A, Takara, Dalian, China). Subsequently, the quality and concentration of extracted RNA was measured using a Nano drop and Agilent 2000 bioanalyzer (Thermo Fisher Scientific, MA, USA).

2.3. RNA sequencing and sanger sequencing

Details of the circRNAs, miRNAs, and mRNAs profile analysis methods are described in Supplementary methods.

To exactly analysis the structure and sequences of hsa_circ_0122319. Sanger sequencing was performed by RiboBio (Guangzhou, China).

2.4. RNase R treatment

Total RNA was incubated for 30 min at 37 °C with 5 U/μg of RNaseR. Then, the expression levels of linear mRNA and hsa_circ_0122319 were detected by qRT-PCR.

2.5. Overexpression of circRNAs

Lentiviral vectors for overexpression of hsa_circ_0122319 constructs were purchased from Hanheng Biotechnology (Shanghai, China). The HUVEC cultured in 6-well plates were infected with lentivirus (MOI = 20, 1*10ˆ8 titers). After infection, the cells were selected with puromycin (1 μg/ml) to generate stable hsa_circ_0122319-expressing. HUVEC infected with empty lentivirus vectors were used as normal control.

2.6. Identification of DE circRNAs, DE miRNAs and DE mRNAs and ceRNAs network construction

RNA-sequencing datasets were analyzed with DEGseq, an R package for screen the differential circRNAs expression using the negative binomial distribution. And a q-value cutoff <0.05 with an absolute $|\log_2 FC| \geq 1$ was used to determine DE circRNAs.

For identification of differential expression levels of miRNAs, normalized data were filtered and the probes marked as detected with 100 % in at least one group were retained for subsequent analyses. To identify DE miRNAs, we screened for miRNAs with the absolute fold change was ≥2.0 during data analysis. For target gene prediction of DE miRNAs, we jointly used three databases (TargetScan-Human 8.0, miRWalk, starBase 2.0). Next, to determine the biological functions or pathways mainly affected by the DE miRNA, GO and KEGG enrichment analysis were performed on the target genes. And differential genes were selected with the same methods described above.

The post-transcriptional regulation of mRNA has been construct based on the interactions among circRNAs, miRNAs and mRNAs. The ceRNAs crosstalk mediated by the same miRNA as a whole is considered as a ceRNAs network. Therefore, we combined our circRNA microarray and miRNA microarray to explore the co-expression of all the DE circRNAs and DE miRNAs. Then, we predicted target genes for each miRNA using TargetscanHuman V8.1, miRWalk and starBase 2.0 database. And we obtained the optimal potential target genes of miRNAs by taking the intersection of the DEGs of mRNA microarray and the target genes prediction of miRNAs. For result of the above, we build ceRNAs network and visualized via Cytoscape (bioinformatic software, V3.8.2). Then, we used CytoHubba plugin in Cytoscape to filter top 10/15 DE RNAs (circRNAs, miRNAs and mRNAs) based on Maximal Clique Centrality (MCC) algorithm [16].

2.7. GO enrichment and KEGG pathway analysis PPI network construction of DEGs

To perform GO enrichment analysis is to know the main activities of gene products at the molecular level and the function of genes in cell [17]. In addition, KEGG pathway enrichment analysis can help us to understand the molecular interaction network in cells and the unique changes of specific organisms [18]. GO enrichment analysis were performed using the "clusterProfiler" [19]and "org.Hs.eg.db" R package and visualized using "GOplot" [20]and "enrichplot" package. KEGG assignments were done using DAVID and were visualized by using Enrich-Bar tools in Hiplot (https://hiplot.com.cn), a comprehensive and easy-to-use web service boosting the publication-ready biomedical data visualization. $P < 0.05$ was considered statistically significant. In addition, the STRING (V11.5, https://string-db.org/) online database was used for the construction and download of the DEGs [21]. And the confidence score≥0.4 was screened to construct the PPI network which was considered the medium confidence score. Then, the PPI network was displayed using Cytoscape software and the most significant modules in the network were identified by the cytohubba plugin [22].

2.8. Quantitative real-time PCR validation

For further validation of identified DE circRNAs, we collected ten peripheral blood samples from coronary heart disease with diabetes and six samples from control patients were collected in Tongji Hospital of Shanghai in june through august 2020. According to manufacturer's instructions, subsequently, the whole blood total RNA extraction kit (SparkJade, Shandong, China, Cat. No: P8610) was used to extract the total RNA from freshly collected whole blood immediately. The extracted total RNA is used for subsequent experiments or stored at −80 °C. qRT-PCR was performed to analyze the genes of interest using the TB Green premix Ex Taq (Tli RNaseH Plus, RR420A, Takara). The expression level of genes was explored using the comparative ct method ($2^{-\Delta\Delta Ct}$). And the primer used in this study are listed in Supplementary Table 1. This study was executed in accordance with the Declaration of Helsinki. Approval was obtained from the Institutional Ethics Committee of the Tongji Hospital, Tongji University (2021-KYSB-121). Informed consent was waived due to the anonymized processing of patients data.

2.9. Western blotting

HUVEC total protein was extracted using RIPA lysis buffer (Epizyme PC101) and centrifuged at 12000 rpm for 10 min at 4 °C. Each sample's total protein was then separated via SDS-PAGE (Epizyme), transferred onto PVDF membranes (Sigma-Aldrich, MO, USA, ISEQ00010), and blocked with 5 % nonfat skim milk (Epizyme, PS112) for 2 h at room temperature. Following blocking, membranes were incubated overnight at 4 °C with primary antibodies: p16 (HUABIO, ER2001-30, 1:1000), p21 (Cell Signaling Technology,

#2946S, 1:1000), p-Phosphatidylinositol-3-kinase (PI3K)-p85α (Abmart, T40116F, 1:1000), PI3K-p85α (Abmart, T40115F, 1:1000), p-Protein Kinase B (Akt) (Abmart, T40068F, 1:1000), Akt (Abmart, T55561F, 1:1000) and GAPDH (Affinity, #T0004, 1:1000). Subsequently, membranes were incubated with corresponding HRP-labeled secondary antibodies (Affinity, #S0002 for anti-mouse, #S0001 for anti-rabbit) at room temperature for 1 h, following three washes with PBS 0.1 % Tween-20. Immunoblots were detected using an enhanced chemiluminescence reagent (ECL), with GAPDH serving as internal controls.

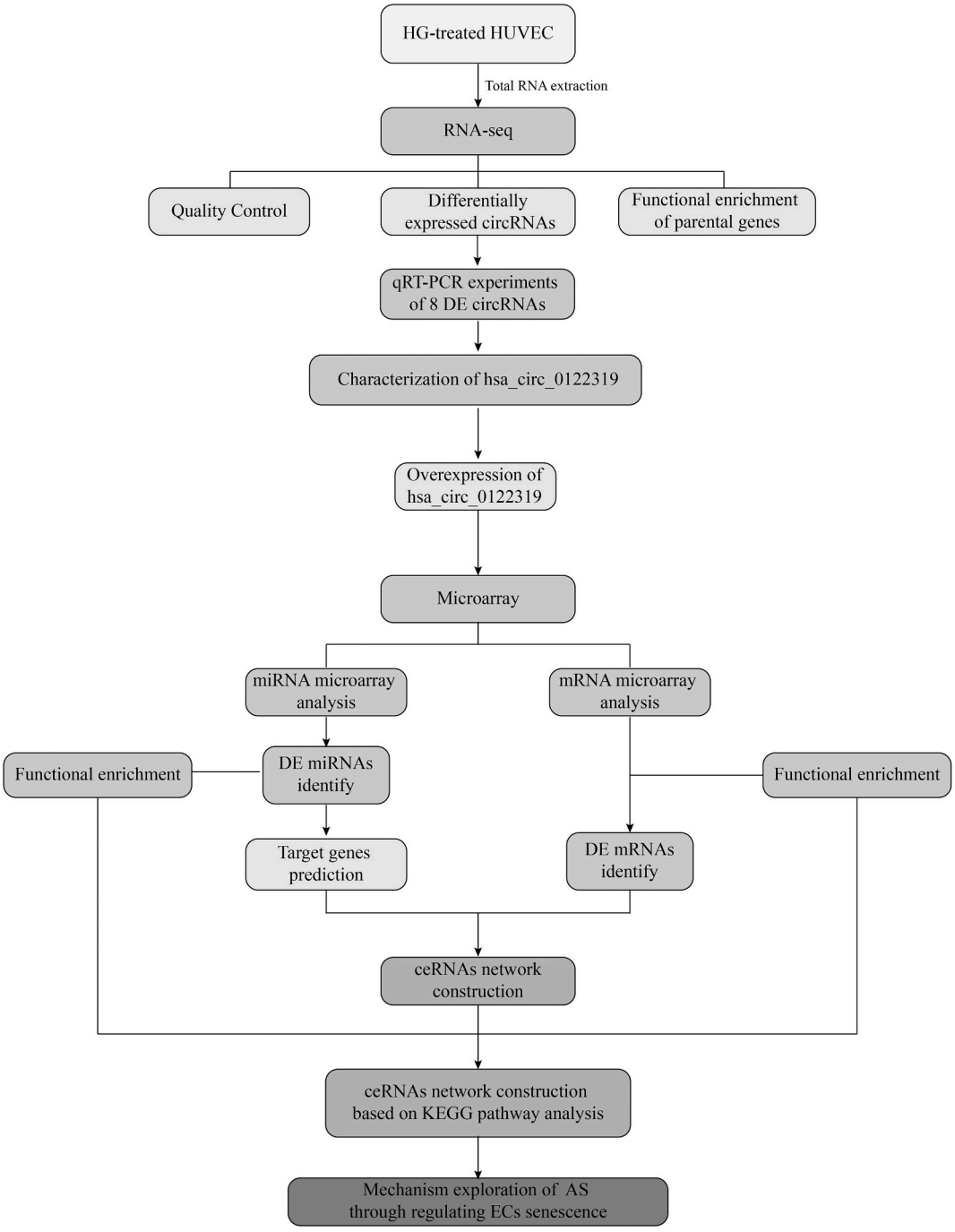

Fig. 1. The workflow of the integrative transcriptomics analyses and experimental validation. HG, high glucose; HUVEC, Human umbilical vein endothelial cell; DE, differentially expressed; ECs, endothelial cells.

2.10. Statistical analysis

All statistical analyses were conducted using the GraphPad Prism 9.0 software. The results are presented as the means ± standard deviation (SDs). In case of multiple comparisons, the data was determined using a one-way ANOVA test. Each experiment was repeated at three times and p values < 0.05 were considered statistically significant.

3. Result

3.1. Overview of whole transcriptome analysis

Initially, we identified differential expression profiles of circRNAs in HG environments by high-throughput sequencing. Quality analysis of raw sequencing data was conducted to assess the suitability for subsequent bioinformatics analysis. On average, the sequencing data exhibited high quality, with over 86 % of high-quality clean reads and an average Q30 percentage exceeding 93 % (Supplementary Table 2). On average, each group exhibited the detection of 1000 known circRNAs and a total of 39,663 circRNAs. The evaluation of miRNA sequencing results revealed a median coefficient of variation (MCV) of approximately 2 % in each group, indicating the accuracy of the sequencing results. The grouping and MCV of mRNA sequencing mirrored those of miRNA sequencing. Fig. 1 illustrates each analysis strategy and the procedures followed in this study.

3.2. Identification of circRNAs in HUVEC treated with HG

In this study, circRNAs were systematically identified and annotated using the DEGseq R package and ANNOVAR software. And a threshold of $|\log_2(FC)| \geq 1$ and Q-value (FDR-corrected p value) < 0.05 was set to define DE circRNAs. Firstly, the DE circRNAs from two groups (NC vs HG-1, NC vs HG-2, collectively named HG group) of samples with identical treatment conditions were merged, and those with smaller Q-values were selected. The volcano plot revealed differential alterations in the expression of 917 circRNAs within

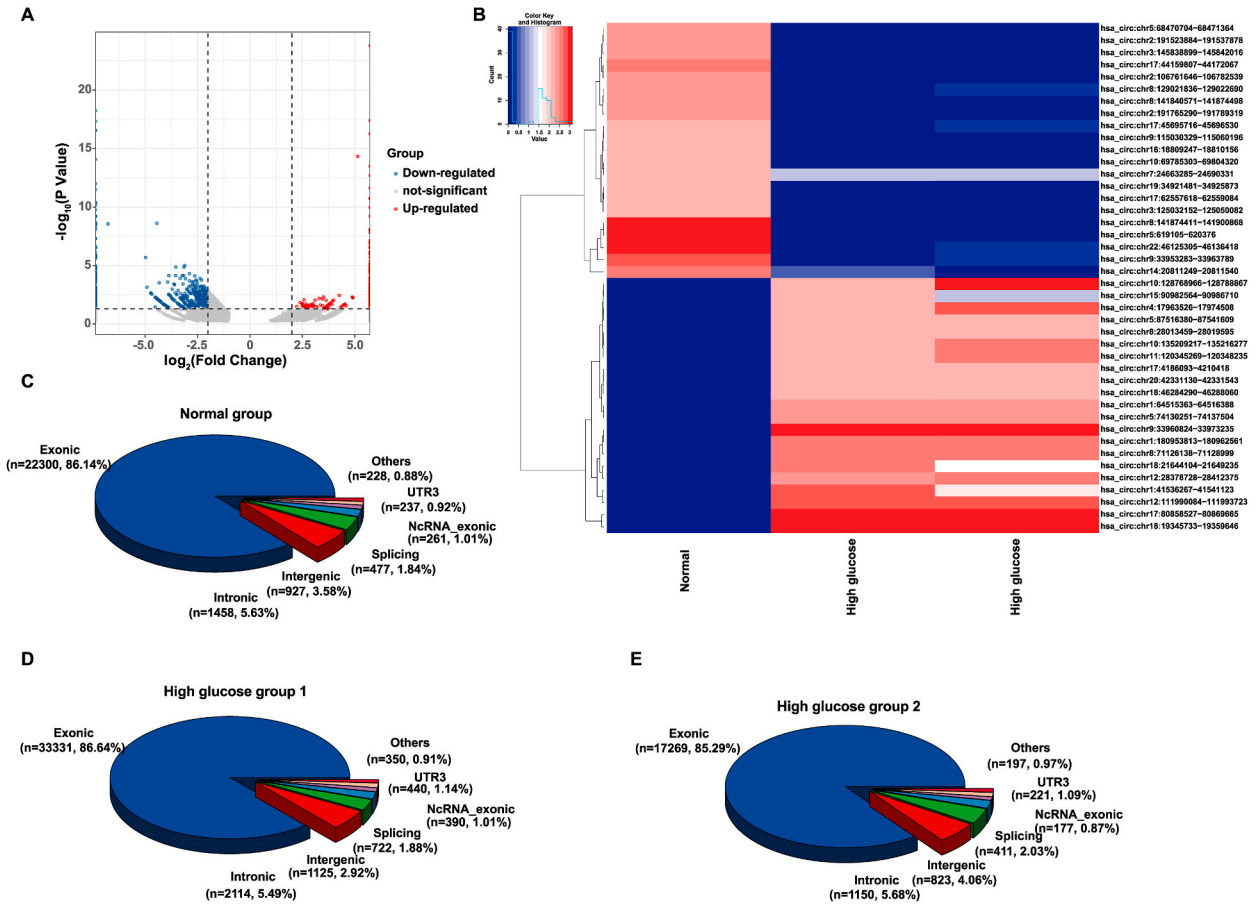

Fig. 2. Identification of DE circRNAs in HG environment. A-B. The volcano plot and heatmap of DE circRNAs in HG group. C-E. The pie chart of the overall distribution difference of the circRNA-seq fragments in the genome between samples. HG, high glucose; DE, differentially expressed.

the HG environment, comprising 301 up-regulated and 616 down-regulated circRNAs (Fig. 2A). Additionally, the heatmap depicted dysregulated circRNAs in HG-induced HUVEC, providing further evidence of the influence of the HG environment on circRNAs expression profiles (Fig. 2B). The positions of the two ends of the circRNAs splicing site on the genome were compared using the ANNOVAR software, and functional elements (exons, introns, splice sites, 5′UTR, 3′UTR, intergenic regions, etc.) were annotated. This process counts the source regions of the sequences at both ends of the circRNAs splicing site, aiding in predicting the source of circRNAs in the genome and obtaining the overall distribution difference of the circRNAs transcription level between samples (Fig. 2C–E).

3.3. Identification and validation of hsa_circ_0122319 in HUVEC

In this study, we identified circRNAs that exhibited differential expression in ECs when exposed to HG conditions. Subsequently, we

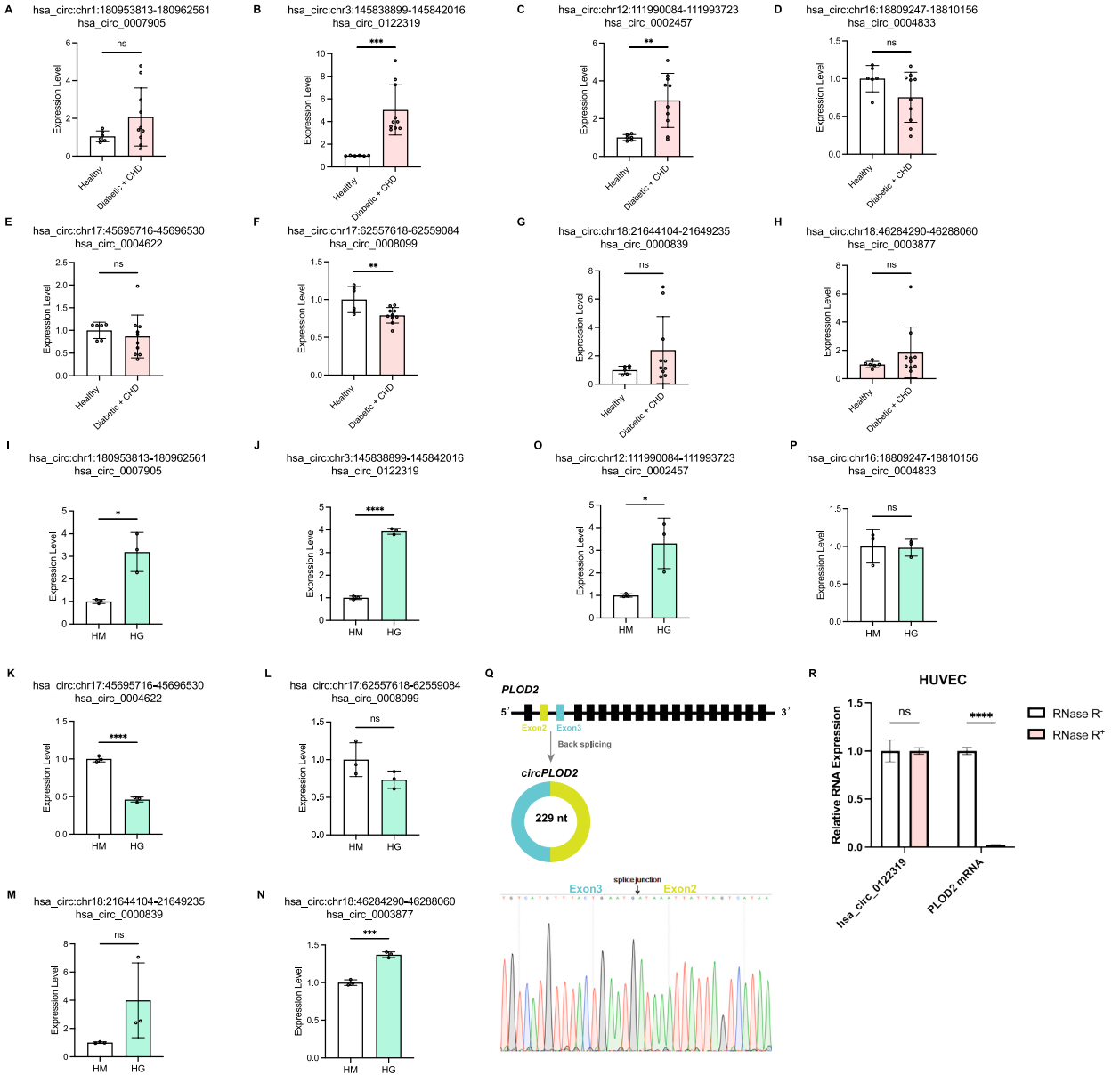

Fig. 3. Identification and validation of DE circRNAs. A-H. Quantitative real-time PCR validation of 8 key circRNAs between coronary heart disease patients with diabetes and normal control. I-P. Quantitative real-time PCR validation of 8 key circRNAs between HG group and normal control. (The values are expressed as mean ± SD from at least two independent experiments, ****P < 0.0001, ***P < 0.001, **P < 0.01, *P < 0.05, ns: no significance) Q. Schematic structure of hsa_circ_0122319, as verified using Sanger sequencing. R. Stability of hsa_circ_0122319 with PLOD2 mRNA was detected in RNase R-treated HUVEC. HG, high glucose; DE, differentially expressed.

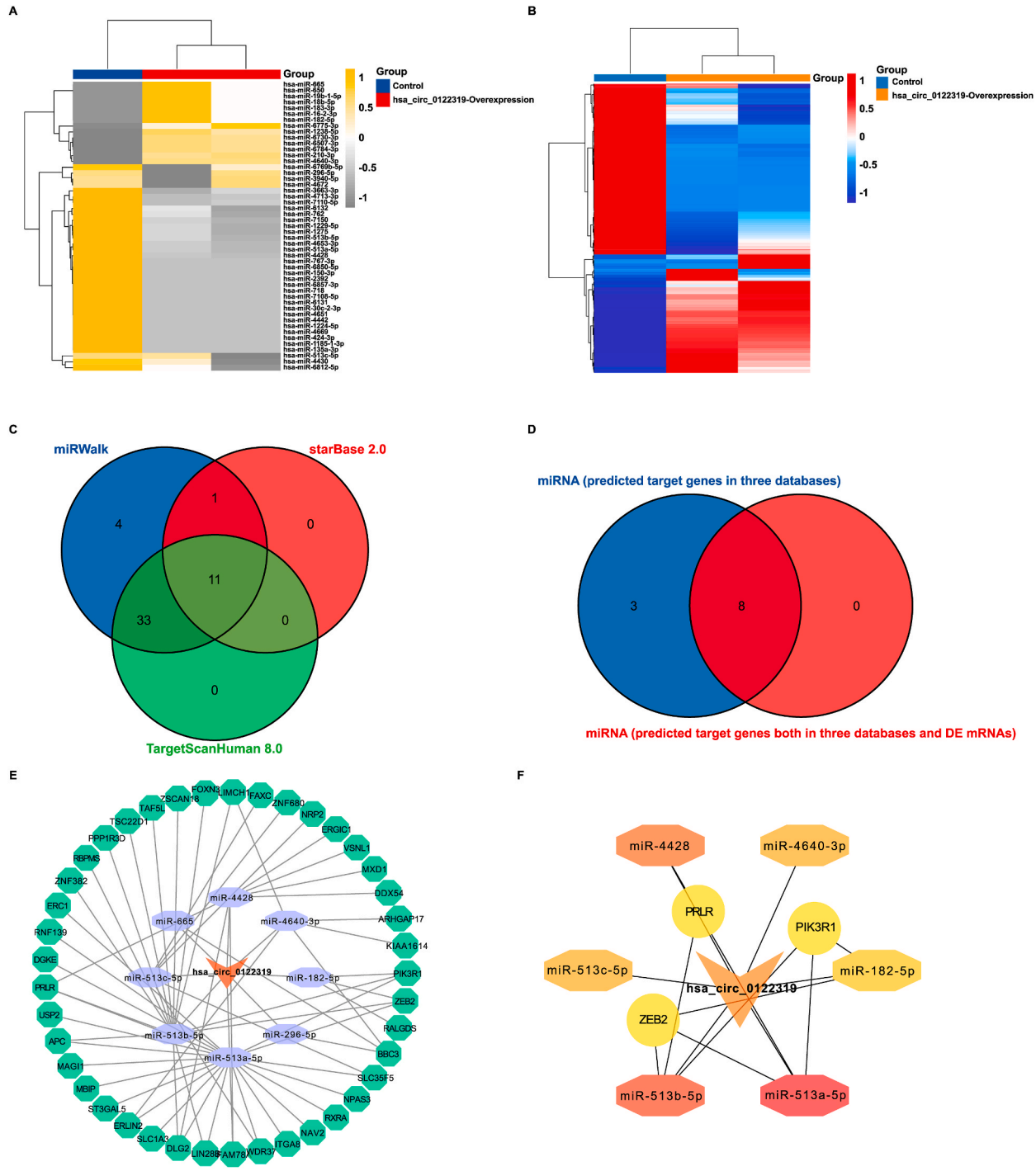

Fig. 4. Identification of DE miRNAs and DE mRNAs in HUVEC after overexpression of hsa_circ_0122319. A-B. Heatmap showed that DE miRNAs and DE mRNAs in microarray analysis and the consistency of expression between samples; C. Venn diagram showed that the number of miRNAs corresponding to downstream target genes that can be predicted in the three databases (49 DE miRNAs). Blue circle represents the miRWalk database, the red circle represents the starBase 2.0 database, and the green circle represents the TargetscanHuman8.0 database; D. Downstream of 11 miRNAs target gene prediction results, these results are then intersected with the DE mRNAs to take the intersection, and the Venn diagram shows the number of intersecting miRNAs. E. ceRNAs network related to hsa_circ_0122319, where orange V-shape represents circRNAs, purple octagon represents miRNAs, and fluorescent green circle represents mRNAs; F. Results of cytoHubba algorithm. cytoHubba identified the hub genes according to the MCC algorithm, where V-shape represents circRNAs, octagon represents miRNAs, circle represents mRNAs, and the color shades represent the ordering of the MCC algorithm, with red representing the top ordering. (For interpretation of the references to color in this figure legend, the reader is referred to the Web version of this article.)

selected the circRNAs that were significantly DE and highly enriched in the KEGG pathway according to the functional pathway correlation analysis. In clinical practice, diabetic patients often suffer from coronary heart disease, and vice versa, coronary heart disease patients often experience the progression of diabetes. There is a bidirectional relationship between the two diseases, which mutually aggravate each other. Therefore, we collected peripheral blood samples from diabetic patients with coronary heart disease and healthy volunteers, respectively, to validate the expression of the screened circRNAs (Fig. 3A–H). In addition, we also performed validation at the cellular level by collecting total RNA from ECs treated with HG (Fig. 3I–P). The qRT-PCR results were basically consistent with the microarray results, but a small part of results with no changes in statistically significance, in addition to experimentally verified hsa_circ_0122319 was found to be opposite to the microarray results. Among the 8 candidates we identified, we selected circRNA (chr3:145838899-145842016) with the most statistical significance for further analysis. And the circRNA ID of above selected circRNA was hsa_circ_0122319. The other 7 circRNAs were hsa_circ_0002457, hsa_circ_0007905, hsa_circ_0004833, hsa_circ_0004622, hsa_circ_0008099, hsa_circ_0000839 and hsa_circ_0003877.

The qRT-PCR results showed that the expression of hsa_circ_0122319 was significantly upregulated in ECs treated with 30 mmol/L D-glucose compared with the control group (Fig. 3B and J). However, the expression of its parental genes did not change significantly (Fig. S2). Moreover, we confirmed the back-spliced junctions of the hsa_circ_0122319 in the RT-PCR products by Sanger sequencing. The results showed that hsa_circ_0122319 (chr3:145838899-145842016) originated from the 2nd and 3rd exon regions of the

Table 1
The differentially expressed miRNAs in hsa_circ_0122319 overexpression group.

miRNA	log_2FC	Regulation
hsa-miR-1185-1-3p	−4.070689	down
hsa-miR-1224-5p	−4.4722905	down
hsa-miR-1229-5p	−1.9180062	down
hsa-miR-1238-5p	1.7762111	up
hsa-miR-1275	−1.3414822	down
hsa-miR-135a-3p	−4.200999	down
hsa-miR-150-3p	−1.8346251	down
hsa-miR-16-2-3p	1.3131342	up
hsa-miR-182-5p	1.3131342	up
hsa-miR-183-3p	1.3131342	up
hsa-miR-18b-5p	1.3131342	up
hsa-miR-19b-1-5p	1.3131342	up
hsa-miR-210-3p	1.4711573	up
hsa-miR-2392	−1.8346251	down
hsa-miR-296-5p	−1.8238685	down
hsa-miR-30c-2-3p	−3.5329309	down
hsa-miR-3663-3p	−1.0596883	down
hsa-miR-3940-5p	−1.68806	down
hsa-miR-424-3p	−3.9403667	down
hsa-miR-4428	−1.0188628	down
hsa-miR-4430	−3.3827877	down
hsa-miR-4442	−4.504717	down
hsa-miR-4640-3p	1.1830566	up
hsa-miR-4651	−3.529074	down
hsa-miR-4653-3p	−1.2955372	down
hsa-miR-4669	−4.462833	down
hsa-miR-4672	−2.1720705	down
hsa-miR-4713-3p	−1.2038729	down
hsa-miR-513a-5p	−1.0319506	down
hsa-miR-513b-5p	−1.3391528	down
hsa-miR-513c-5p	−2.0841882	down
hsa-miR-6131	−3.5501153	down
hsa-miR-6132	−1.0235977	down
hsa-miR-650	1.3131342	up
hsa-miR-6507-3p	1.042717	up
hsa-miR-665	1.3131342	up
hsa-miR-6730-3p	3.7232637	up
hsa-miR-6769b-5p	−3.1447048	down
hsa-miR-6775-3p	1.4546824	up
hsa-miR-6784-3p	1.0016675	up
hsa-miR-6812-5p	−1.9220757	down
hsa-miR-6850-5p	−1.8346251	down
hsa-miR-6857-3p	−2.759679	down
hsa-miR-7108-5p	−3.5891683	down
hsa-miR-7110-5p	−1.3815979	down
hsa-miR-7150	−1.0314455	down
hsa-miR-718	−3.6536064	down
hsa-miR-762	−1.091434	down
hsa-miR-767-3p	−1.8346251	down

procollagen-lysine,2-oxoglutarate 5-dioxygenase 2 (PLOD2) gene (Fig. 3Q). In addition, as shown in Fig. 3R, hsa_circ_0122319 was resistant to RNase R, while linear RNA PLOD2 could be digested by RNase R, indicating that hsa_circ_0122319 harbor a loop structure. Collectively, these results confirmed that hsa_circ_0122319 possess the characteristics of circular RNA, and suggested that its functions may benefit from the biostability of this type of molecule.

3.4. Identification of DE miRNAs and DE mRNAs in HUVEC after overexpression of hsa_circ_0122319

To investigate the effect of hsa_circ_01222319 on the expression of miRNAs and mRNAs in HUVEC, we performed mioarray analysis after overexpressing hsa_circ_01222319 in HUVEC. We identified 49 DE miRNAs and 459 DE mRNAs. Among them, 14 miRNAs and 188 mRNAs were up-regulated, while 35 miRNAs and 271 mRNAs were down-regulated by hsa_circ_01222319 overexpression. The volcano plots and heatmaps of the DE miRNAs and DE mRNAs are shown in Fig. 4A and B, respectively. Total of miRNAs and mRNAs are listed in Table 1 and Supplementary Table 4, respectively.

3.5. Target genes prediction of DE miRNAs

We predicted target genes of DE miRNAs by using three databases: miRWalk database [23], TargetscanHuman8.0 database [24] and starBase V2.0 database [25]. Among them, there were a total of 11 miRNAs whose downstream target genes could be predicted in

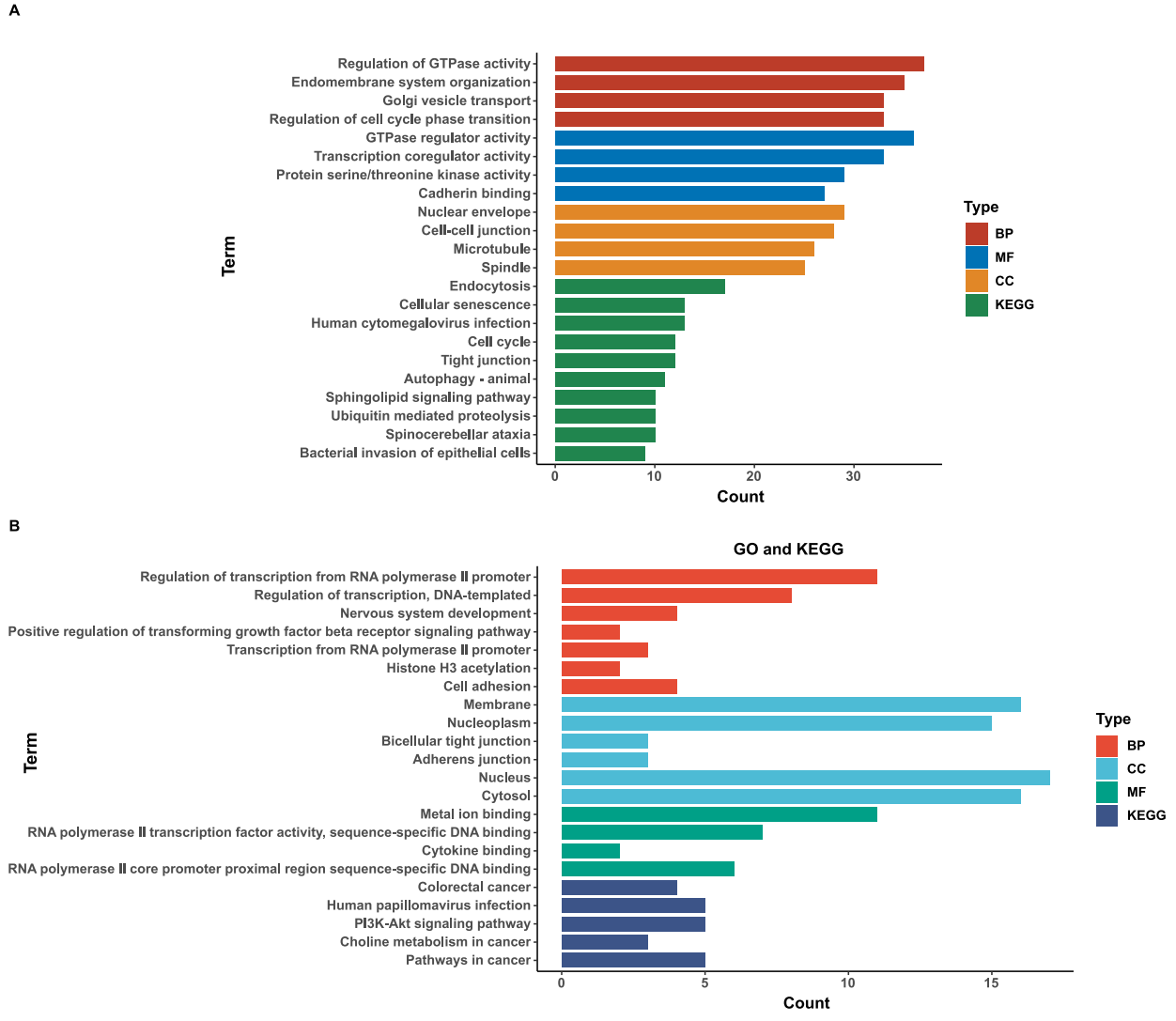

Fig. 5. GO and KEGG pathway analysis. A. The top 12 highest enriched gene GO terms and top 10 enriched KEGG pathways for parental genes of DE circRNAs in the HG environment. B. Bar graph showed that the top 7 results of GO and KEGG pathway enrichment analysis of mRNAs in the ceRNAs network.

all the above three databases (Fig. 4C). Additionally, considering that circRNAs may concurrently regulate the expression of downstream target genes of differential miRNAs, and to further improve the credibility of the prediction results. We analyzed the overlap between the predicted downstream target genes of these 11 miRNAs and the DE mRNAs resulting from hsa_circ_0122319 overexpression. Our result revealing that 8 of the miRNAs' predicted target genes overlapped with DE mRNAs (Fig. 4D).

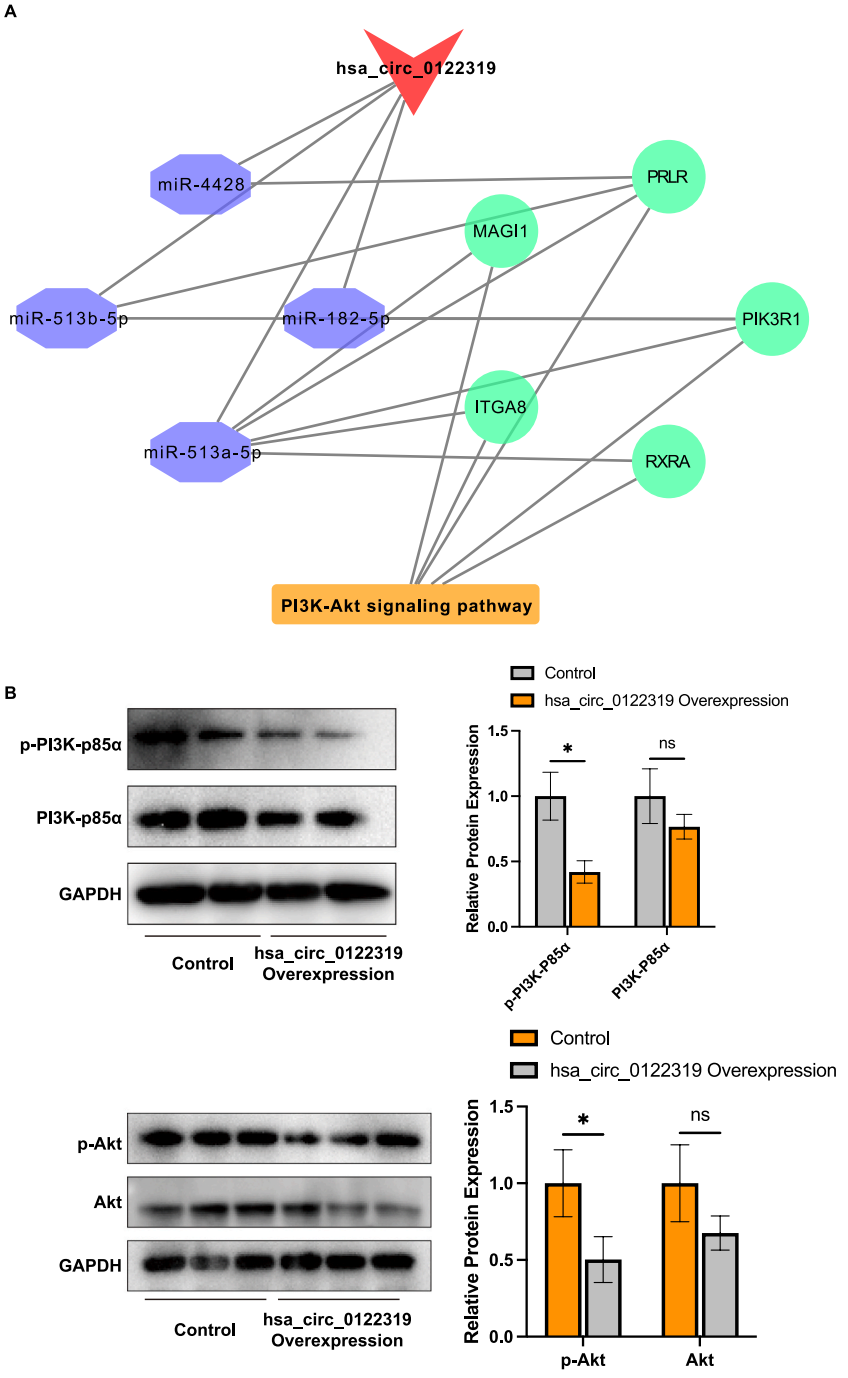

Fig. 6. The ceRNAs network construction. A. CeRNAs network related to PI3K-Akt signaling pathway, where red V shapes represent circRNAs, purple octagons represent miRNAs, fluorescent green circles represent mRNAs, and orange rectangles represent pathway. B. Western blot analysis was employed to assess the PI3K/Akt pathway protein expression in endothelial cells after overexpression of hsa_circ_0122319. Control was the lentivirus transfection control, hsa_circ_0122319 overexpression was the hsa_circ_0122319 overexpression group. ns stands for no statistically significant difference, * indicates $p < 0.05$. (For interpretation of the references to color in this figure legend, the reader is referred to the Web version of this article.)

3.6. Construction of circRNA-miRNA-mRNA network

To investigate the potential regulatory mechanisms of the DE circRNAs in HUVEC under HG condition, we constructed a circRNA-miRNA-mRNA network based on the predicted interactions between the DE circRNAs, their corresponding miRNAs and the DE mRNAs. Firstly, we constructed a 1 DE circRNA, 8 DE miRNAs and 41 mRNAs ceRNAs network related to hsa_circ_0122319. And the circRNA-miRNA-mRNA network was visualized by Cytoscape software (Fig. 4E). Then, the CytoHubba plug-in revealed that the top 10 miRNAs and mRNAs related to ceRNAs network of hsa_circ_0122319 (Fig. 4F) by the degree algorithm. The network showed that hsa_circ_01222319 had multiple miRNAs response elements (MREs) and could interact with several miRNAs, suggesting that they might act as important regulators in HUVEC under HG condition.

3.7. Functional enrichment and pathway analysis

Functional enrichment analysis was performed to explore the enrichment pathways of parental genes of DE circRNAs, DE mRNAs and target genes of DE miRNAs. Firstly, we investigated the parent genes of DE circRNAs by enrichment analysis. We found these parent genes mainly enriched in regulation of GTPase activity and regulation of cell cycle phase transition in biological processes (BP). The cellular component (CC) consisted of nuclear envelope and cell-cell junction. And the molecular function (MF) included transcription coregulator activity and protein serine/threonine kinase activity. In addition, KEGG pathway mainly enriched in senescence pathways, such as endocytosis, cellular senescence, human cytomegalovirus infection and cell cycle (Fig. 5A).

Thereafter, we analyzed the mRNAs in the ceRNAs network for functional enrichment. The results showed that these genes were mainly enriched at the key BP such as regulation of RNA polymerase II promoter transcription, transcriptional regulation on DNA templates, development of the nervous system, positive regulation of the transforming growth factor β receptor signaling pathway, transcription of RNA polymerase II promoter, and acetylation of histone H3. In terms of CC, the significantly enriched terms include the nuclear envelope and intercellular junctions. In terms of MF, these mRNAs showed strong correlation for functions such as metal ion binding, RNA polymerase II transcription factor activity, sequence-specific DNA binding and cytokine binding. Further KEGG pathway analysis revealed significant enrichment of these genes in colorectal cancer, human papillomavirus infection, PI3K-Akt signaling pathway, choline metabolism, and pathways associated with cancer development, indicating possible key regulatory roles of the ceRNAs network in these biological processes and disease pathways (Fig. 5B). These findings provide important biological insights for further understanding the role of the ceRNAs network in cellular physiology and disease mechanisms.

3.8. Construction of ceRNAs network in PI3K-Akt signaling pathway

Meanwhile, the above KEGG pathway enrichment analysis revealed that the genes in the ceRNAs network were significantly enriched in the PI3K-Akt signaling pathway, and several studies suggested that the PI3K-Akt pathway was closely related to ECs senescence. Therefore, we further constructed a ceRNA network associated with the PI3K-Akt pathway (Fig. 6A). This network analysis revealed several key nodes and regulatory axes that may play critical roles in the PI3K-Akt pathway. In addition, Western blot experiments preliminarily confirmed that overexpression of hsa_circ_0122319 downregulated the expression of phosphorylated PI3K-p85 and phosphorylated Akt proteins (Fig. 6B). This indicates that hsa_circ_0122319 may inhibit the activation of the PI3K/Akt pathway. Previous studies have shown that the PI3K/Akt pathway is involved in the regulation of cell proliferation and affects nitric oxide (NO) content by mediating the phosphorylation of endothelial nitric oxide synthase (eNOS), which in turn exerts anti-senescence effects [26,27]. Thus, we suggest that hsa_circ_0122319 may be involved in regulating endothelial senescence through the PI3K/Akt pathway. It also provides a reference for future exploration of multiple molecular pathways of ECs senescence.

4. Discussion

AS is a multiple factor-involved chronic inflammatory disease in the arterial wall, and is the dominant cause of cardiovascular disease [28]. Moreover, the aberrant phenotypic alterations and transformation of ECs induced by HG play crucial roles in initiating AS [29,30]. Recently, there has been a significant focus on identifying novel therapeutic targets and mechanisms for treating AS, primarily centered on lncRNAs, miRNAs, and protein-coding genes [31–33]. Interestingly, a growing body of evidence indicates that circRNAs may serve as novel biomarkers for various diseases [34]. circRNAs exerted a crucial part in ceRNAs network and circRNA-miRNA-mRNA crosstalk. This crosstalk may regulate various physiological and pathophysiological processes at the post-transcriptional level.

Comprehensive RNA expression profiling affords novel opportunities for discovering novel circRNAs and miRNAs. In this study, we identified the differential expression profile of circRNAs in HUVEC subjected to a HG environment, screening 917 circRNAs with differential expression. Then, we performed GO enrichment and KEGG pathway analysis for the parental genes of DE circRNAs in HG group. We found that the enriched terms of parental genes of DE circRNAs were associated with the progression of AS. The enriched terms consisted of cell-cell junction [35], endocytosis [36], cell cycle [37] and cellular senescence [38] were important biological process or molecular pathways in AS. To further clarify which circRNAs function among the DE circRNAs in HG environments and by what mechanism. We selected eight candidate circRNAs for further validation by integrating significantly upregulated and down-regulated circRNAs identified through high-throughput sequencing and those highly enriched in the KEGG pathway. According to the results of qRT-PCR, we observed significant changes in expression for hsa_circ_0122319. Different levels of expression of circRNAs have been reported to have crucial roles in formation of atherosclerotic plaque [13,39,40]. For instance, as a miRNA sponge, circRSF1

may delay the progression of AS by inhibiting ox-LDL-induced endothelial proliferation and inflammation through miR-135b-5p/HDAC1 axis [41]. It was also found that circ_0044073 could promote proliferation and invasion of HUVECs and VSMCs through miR-107/JAK/STAT pathway participate in the progression of AS [42]. In our present study, our results indicated elevated hsa_circ_0122319 expression in HG-treated HUVEC as well as the plasma of CHD patients with diabetes. Additionally, we demonstrated that hsa_circ_0122319 not only served as an independent risk factor for AS pathogenesis but also exhibited potential diagnostic value for AS. Consequently, we selected hsa_circ_0122319 for subsequent miRNA and mRNA microarray analysis.

Multiple classes of RNA profiles may facilitate the prediction of ceRNAs networks in the development of AS. Previous studies have demonstrated that circRNAs, which are enriched for miRNA seeds, may perform their function mainly by acting as miRNA sponges. Therefore, we identified the differential expression profiles of miRNAs and mRNAs after overexpression of hsa_circ_0122319 by microarray analysis. Our understanding of miRNA regulatory mechanisms has been of greatly expanded by recent studies of the ceRNAs network and crosstalk. Thus, we built a ceRNAs network consisting of 1 circRNA, 8 miRNAs and 41 mRNAs. To our knowledge, this is the first time that both miRNAs and mRNAs differential expression profiles downstream of hsa_circ_0122319 were identified, and the first time that a ceRNAs network dominated by hsa_circ_0122319 was constructed. Several miRNAs in the network are known as regulators of glucose metabolism or CVD. MiRNAs exhibit various roles in multiple biological processes of many diseases, previous study has shown that miR-182-5p can inhibit oxidative stress and apoptosis via inactivating TLR4 expression in regulation of AS [43]. Furthermore, certain miRNAs, such as miR-513a-5p [44] and miR-513c-5p [45], along with their target genes, have been implicated in potentially regulating ECs function. But the other miRNA's potential role in AS has not been explored. Therefore, this issue can be investigated in future follow-up studies.

The ceRNAs network not only reveals the interaction relationship between miRNAs and mRNAs, but also provides a basis for further functional and pathway enrichment analysis. By analyzing the GO and KEGG pathway enrichment of mRNAs in the ceRNAs network, we identified several important pathways related to cell function regulation, inflammatory response and cellular aging, especially the activity of the PI3K-Akt pathway was significantly affected. PI3K-Akt pathway, as a key network for cell signaling, plays an important role in regulating cell growth, proliferation, survival and metabolism. metabolism and other physiological processes. Activation of this pathway begins with activation of PI3K, followed by activation of the serine/threonine kinase Akt via phosphorylation, which in turn regulates multiple downstream targets, including mTOR, that are critical for cell cycle and apoptosis [46]. Liu et al. found that MEF2A protects against vascular ECs senescence via increase the level the of SIRT1 through PI3K-Akt signaling pathway [47]. In addition, PI3K-Akt pathway involved in the formation of AS by regulating autophagy [48,49]. Together, the above studies highlight the critical role of the PI3K-Akt pathway in mediating aging in ECs senescence and its potential as a target for therapeutic intervention in diseases characterized by vascular aging and dysfunction. In future studies, the impact of this mechanism in progression of AS can be further explored based on the hsa_circ_0122319-mediated PI3K-Akt pathway and ceRNAs network.

Meanwhile, our study has certain limitations. Firstly, the expression level of hsa_circ_0122319 validated by our experiments contradicted the preliminary high-throughput sequencing results. This finding triggered us to think deeply about the experimental design and data interpretation, as well as to explore the possible mechanisms. This discrepancy may stem from the sample selection and handling process of heterogeneity. High-throughput sequencing relies on complex bioinformatics analysis, and both the biological differences between different samples and the number of sequenced samples can have an impact on the bias of the results. In this study, the number of sequenced samples in this experiment was relatively small due to insufficient funding at the time of sequencing and other reasons, which may also lead to the bias of the results. However, high-throughput sequencing and biosignature analysis are only the main research targets to show the differentially expressed circRNAs profiles under different condition treatments as well as to screen out the regulatory disease phenotypes. In our study, we successfully screened hsa_circ_0122319 as a subsequent research target after the validation of bioinformatics analysis and in vitro experiments to achieve the initial purpose of high-throughput sequencing.

In addition, experimental verification is needed for screened miRNAs and mRNAs, just as an in-depth exploration of DE circRNAs. Likewise, it is also important to identify the specific functions of the ceRNAs networks constructed in this study and place them in the larger background of AS progression. Finally, future studies could focus on validating in larger samples from patients with AS or myocardial infarction, so that risk ratios of candidate molecules can be analyzed, and meaningful AS biomarkers can be utilized in clinical diagnostic and therapeutic targets.

5. Conclusion

We first analyzed the differential expression profiles of circRNAs in HUVEC under HG environment by high-throughput sequencing and further described the differential expression patterns of miRNAs and mRNAs after overexpression of hsa_circ_0122319 by microarray analysis. This is the first study to systematically characterize the dysregulation of circRNA-associated ceRNAs network in ECs under HG environment. In addition, ceRNAs networks associated with the PI3K-Akt signaling pathway were constructed based on functional analysis.

Further studies on the functions of the above molecules and their interactions with circRNAs in the future may contribute to a better understanding of the intrinsic mechanisms of ECs dysfunction and AS and their progression. Finally, the cecRNAs network screened in this study provides additional evidence for subsequent basic research on AS.

Funding

This study was supported by the National Natural Science Foundation of China (Grant No. 82170346), Grant of Shanghai Science and Technology Committee (NO.19XD1403300 and 19411963200) and Shanghai Municipal Health Commission (NO.2019LJ10).

Ethics approval and consent to participate

This study was executed in accordance with the Declaration of Helsinki. Approval was obtained from the Institutional Ethics Committee of The TongJi Hospital, TongJi University (2021-KYSB-121). Informed consent was waived due to the anonymized processing of patient data.

Consent for publication

All authors consent to the publication of the article.

Availability of data and materials

The data generated and analyzed during this study have been deposited in the Gene Expression Omnibus (GEO) database. The dataset is publicly available and can be accessed using the following details:

GEO Accession Number: GSE205264.

Direct URL: https://www.ncbi.nlm.nih.gov/geo/query/acc.cgi?acc=GSE205264.

CRediT authorship contribution statement

Hao Lin: Writing – original draft, Software, Methodology, Data curation. **Tongqing Yao:** Writing – original draft, Project administration, Methodology, Formal analysis. **Haoran Ding:** Software, Methodology, Investigation. **Jiapeng Chu:** Software, Methodology. **Deqiang Yuan:** Visualization, Software. **Fan Ping:** Validation, Formal analysis. **Fei Chen:** Writing – review & editing, Validation, Supervision, Formal analysis, Conceptualization. **Xuebo Liu:** Writing – review & editing, Validation, Supervision, Funding acquisition, Data curation, Conceptualization.

Declaration of competing interest

The authors declare that they have no known competing financial interests or personal relationships that could have appeared to influence the work reported in this paper.

Acknowledgements

We thank Dr.Jianming Zeng(University of Macau), and all the members of his bioinformatics team, biotrainee, for generously sharing their experience and codes.

Appendix A. Supplementary data

Supplementary data to this article can be found online at https://doi.org/10.1016/j.heliyon.2024.e37028.

References

[1] Diagnosis and classification of diabetes mellitus, Diabetes Care 36 (Suppl 1) (2013) S67–S74. Suppl 1.
[2] N. Tang, S. Jiang, Y. Yang, S. Liu, M. Ponnusamy, H. Xin, T. Yu, Noncoding RNAs as therapeutic targets in atherosclerosis with diabetes mellitus, Cardiovasc Ther 36 (4) (2018) e12436.
[3] F. Tang, T.L. Yang, MicroRNA-126 alleviates endothelial cells injury in atherosclerosis by restoring autophagic flux via inhibiting of PI3K/Akt/mTOR pathway, Biochem. Biophys. Res. Commun. 495 (1) (2018) 1482–1489.
[4] N. Sawada, A. Jiang, F. Takizawa, A. Safdar, A. Manika, Y. Tesmenitsky, K.T. Kang, J. Bischoff, H. Kalwa, J.L. Sartoretto, et al., Endothelial PGC-1α mediates vascular dysfunction in diabetes, Cell Metab 19 (2) (2014) 246–258.
[5] F. Liu, S. Fang, X. Liu, J. Li, X. Wang, J. Cui, T. Chen, Z. Li, F. Yang, J. Tian, et al., Omentin-1 protects against high glucose-induced endothelial dysfunction via the AMPK/PPARδ signaling pathway, Biochem. Pharmacol. 174 (2020) 113830.
[6] J.A. Beckman, M.A. Creager, P. Libby, Diabetes and atherosclerosis: epidemiology, pathophysiology, and management, JAMA 287 (19) (2002) 2570–2581.
[7] J.A. Beckman, F. Paneni, F. Cosentino, M.A. Creager, Diabetes and vascular disease: pathophysiology, clinical consequences, and medical therapy: part II, Eur. Heart J. 34 (31) (2013) 2444–2452.
[8] L.S. Kristensen, M.S. Andersen, L.V.W. Stagsted, K.K. Ebbesen, T.B. Hansen, J. Kjems, The biogenesis, biology and characterization of circular RNAs, Nat. Rev. Genet. 20 (11) (2019) 675–691.
[9] S. Qu, Y. Zhong, R. Shang, X. Zhang, W. Song, J. Kjems, H. Li, The emerging landscape of circular RNA in life processes, RNA Biol. 14 (8) (2017) 992–999.
[10] J. Greene, A.M. Baird, L. Brady, M. Lim, S.G. Gray, R. McDermott, S.P. Finn, Circular RNAs: biogenesis, function and role in human diseases, Front. Mol. Biosci. 4 (2017) 38.
[11] L. Salmena, L. Poliseno, Y. Tay, L. Kats, P.P. Pandolfi, A ceRNA hypothesis: the Rosetta Stone of a hidden RNA language? Cell 146 (3) (2011) 353–358.
[12] S. Zhang, G. Song, J. Yuan, S. Qiao, S. Xu, Z. Si, Y. Yang, X. Xu, A. Wang, Circular RNA circ_0003204 inhibits proliferation, migration and tube formation of endothelial cell in atherosclerosis via miR-370-3p/TGFβR2/phosph-SMAD3 axis, J. Biomed. Sci. 27 (1) (2020) 11.
[13] F. Zhang, R. Zhang, X. Zhang, Y. Wu, X. Li, S. Zhang, W. Hou, Y. Ding, J. Tian, L. Sun, et al., Comprehensive analysis of circRNA expression pattern and circRNA-miRNA-mRNA network in the pathogenesis of atherosclerosis in rabbits, Aging (Albany NY) 10 (9) (2018) 2266–2283.

[14] L. Yang, F. Yang, H. Zhao, M. Wang, Y. Zhang, Circular RNA circCHFR facilitates the proliferation and migration of vascular smooth muscle via miR-370/FOXO1/cyclin D1 pathway, Mol. Ther. Nucleic Acids 16 (2019) 434–441.
[15] X. Jin, Y. Guan, H. Sheng, Y. Liu, Crosstalk in competing endogenous RNA network reveals the complex molecular mechanism underlying lung cancer, Oncotarget 8 (53) (2017) 91270–91280.
[16] C.H. Chin, S.H. Chen, H.H. Wu, C.W. Ho, M.T. Ko, C.Y. Lin, cytoHubba: identifying hub objects and sub-networks from complex interactome, BMC Syst. Biol. 8 (Suppl 4) (2014) S11. Suppl 4.
[17] Gene ontology consortium: going forward, Nucleic Acids Res. 43 (Database issue) (2015) D1049–1056.
[18] M. Kanehisa, M. Furumichi, M. Tanabe, Y. Sato, K. Morishima, KEGG: new perspectives on genomes, pathways, diseases and drugs, Nucleic Acids Res. 45 (D1) (2017) D353–d361.
[19] G. Yu, L.G. Wang, Y. Han, Q.Y. He, clusterProfiler: an R package for comparing biological themes among gene clusters, OMICS 16 (5) (2012) 284–287.
[20] W. Walter, F. Sánchez-Cabo, M. Ricote, GOplot: an R package for visually combining expression data with functional analysis, Bioinformatics 31 (17) (2015) 2912–2914.
[21] D. Szklarczyk, A.L. Gable, K.C. Nastou, D. Lyon, R. Kirsch, S. Pyysalo, N.T. Doncheva, M. Legeay, T. Fang, P. Bork, et al., The STRING database in 2021: customizable protein-protein networks, and functional characterization of user-uploaded gene/measurement sets, Nucleic Acids Res. 49 (D1) (2021) D605–d612.
[22] P. Shannon, A. Markiel, O. Ozier, N.S. Baliga, J.T. Wang, D. Ramage, N. Amin, B. Schwikowski, T. Ideker, Cytoscape: a software environment for integrated models of biomolecular interaction networks, Genome Res. 13 (11) (2003) 2498–2504.
[23] C. Sticht, C. De La Torre, A. Parveen, N. Gretz, miRWalk: an online resource for prediction of microRNA binding sites, PLoS One 13 (10) (2018) e0206239.
[24] S.E. McGeary, K.S. Lin, C.Y. Shi, T.M. Pham, N. Bisaria, G.M. Kelley, D.P. Bartel, The biochemical basis of microRNA targeting efficacy, Science 366 (6472) (2019).
[25] J.H. Li, S. Liu, H. Zhou, L.H. Qu, J.H. Yang, starBase v2.0: decoding miRNA-ceRNA, miRNA-ncRNA and protein-RNA interaction networks from large-scale CLIP-Seq data, Nucleic Acids Res. 42 (Database issue) (2014) D92–97.
[26] L. Gu, D. Lian, Y. Zheng, W. Zhou, J. Gu, X. Liu, Echinacoside-induced nitric oxide production in endothelial cells: roles of androgen receptor and the PI3K-Akt pathway, Int. J. Mol. Med. 45 (4) (2020) 1195–1202.
[27] H. Niu, J. Li, H. Liang, G. Wu, M. Chen, Exogenous hydrogen sulfide activates PI3K/Akt/eNOS pathway to improve replicative senescence in human umbilical vein endothelial cells, Cardiol. Res. Pract. 2023 (2023) 7296874.
[28] J. Frostegård, Immunity, atherosclerosis and cardiovascular disease, BMC Med. 11 (2013) 117.
[29] M.A. Gimbrone Jr., García-cardeña G: **endothelial cell dysfunction and the pathobiology of atherosclerosis**, Circ. Res. 118 (4) (2016) 620–636.
[30] X. Zhao, L. Su, X. He, B. Zhao, J. Miao, Long noncoding RNA CA7-4 promotes autophagy and apoptosis via sponging MIR877-3P and MIR5680 in high glucose-induced vascular endothelial cells, Autophagy 16 (1) (2020) 70–85.
[31] F.X. Guo, Q. Wu, P. Li, L. Zheng, S. Ye, X.Y. Dai, C.M. Kang, J.B. Lu, B.M. Xu, Y.J. Xu, et al., The role of the LncRNA-FA2H-2-MLKL pathway in atherosclerosis by regulation of autophagy flux and inflammation through mTOR-dependent signaling, Cell Death Differ. 26 (9) (2019) 1670–1687.
[32] Y. Lu, T. Thavarajah, W. Gu, J. Cai, Q. Xu, Impact of miRNA in atherosclerosis, Arterioscler. Thromb. Vasc. Biol. 38 (9) (2018) e159–e170.
[33] M. Iida, S. Harada, T. Takebayashi, Application of metabolomics to epidemiological studies of atherosclerosis and cardiovascular disease, J Atheroscler Thromb 26 (9) (2019) 747–757.
[34] M. Lei, G. Zheng, Q. Ning, J. Zheng, D. Dong, Translation and functional roles of circular RNAs in human cancer, Mol. Cancer 19 (1) (2020) 30.
[35] S. Sivasinprasasn, N. Wikan, J. Tocharus, W. Chaichompoo, A. Suksamrarn, C. Tocharus, Pelargonic acid vanillylamide and rosuvastatin protect against oxidized low-density lipoprotein-induced endothelial dysfunction by inhibiting the NF-κB/NLRP3 pathway and improving cell-cell junctions, Chem. Biol. Interact. 345 (2021) 109572.
[36] Y. Kojima, J.P. Volkmer, K. McKenna, M. Civelek, A.J. Lusis, C.L. Miller, D. Direnzo, V. Nanda, J. Ye, A.J. Connolly, et al., CD47-blocking antibodies restore phagocytosis and prevent atherosclerosis, Nature 536 (7614) (2016) 86–90.
[37] B.G. Childs, M. Gluscevic, D.J. Baker, R.M. Laberge, D. Marquess, J. Dananberg, J.M. van Deursen, Senescent cells: an emerging target for diseases of ageing, Nat. Rev. Drug Discov. 16 (10) (2017) 718–735.
[38] J.C. Wang, M. Bennett, Aging and atherosclerosis: mechanisms, functional consequences, and potential therapeutics for cellular senescence, Circ. Res. 111 (2) (2012) 245–259.
[39] F. Yu, Y. Zhang, Z. Wang, W. Gong, C. Zhang, Hsa_circ_0030042 regulates abnormal autophagy and protects atherosclerotic plaque stability by targeting eIF4A3, Theranostics 11 (11) (2021) 5404–5417.
[40] L.L. Zhang, CircRNA-PTPRA promoted the progression of atherosclerosis through sponging with miR-636 and upregulating the transcription factor SP1, Eur. Rev. Med. Pharmacol. Sci. 24 (23) (2020) 12437–12449.
[41] X. Zhang, J. Lu, Q. Zhang, Q. Luo, B. Liu, CircRNA RSF1 regulated ox-LDL induced vascular endothelial cells proliferation, apoptosis and inflammation through modulating miR-135b-5p/HDAC1 axis in atherosclerosis, Biol. Res. 54 (1) (2021) 11.
[42] L. Shen, Y. Hu, J. Lou, S. Yin, W. Wang, Y. Wang, Y. Xia, W. Wu, CircRNA-0044073 is upregulated in atherosclerosis and increases the proliferation and invasion of cells by targeting miR-107, Mol. Med. Rep. 19 (5) (2019) 3923–3932.
[43] S.B. Qin, D.Y. Peng, J.M. Lu, Z.P. Ke, MiR-182-5p inhibited oxidative stress and apoptosis triggered by oxidized low-density lipoprotein via targeting toll-like receptor 4, J. Cell. Physiol. 233 (10) (2018) 6630–6637.
[44] S. Shin, K.C. Moon, K.U. Park, E. Ha, MicroRNA-513a-5p mediates TNF-α and LPS induced apoptosis via downregulation of X-linked inhibitor of apoptotic protein in endothelial cells, Biochimie 94 (6) (2012) 1431–1436.
[45] C. Chu, B. Wang, Z. Zhang, W. Liu, S. Sun, G. Liang, X. Zhang, H. An, R. Wei, X. Zhu, et al., miR-513c-5p suppression aggravates pyroptosis of endothelial cell in deep venous thrombosis by promoting caspase-1, Front. Cell Dev. Biol. 10 (2022) 838785.
[46] M. Koide, K. Ikeda, Y. Akakabe, Y. Kitamura, T. Ueyama, S. Matoba, H. Yamada, M. Okigaki, H. Matsubara, Apoptosis regulator through modulating IAP expression (ARIA) controls the PI3K/Akt pathway in endothelial and endothelial progenitor cells, Proc Natl Acad Sci U S A 108 (23) (2011) 9472–9477.
[47] B. Liu, L. Wang, W. Jiang, Y. Xiong, L. Pang, Y. Zhong, C. Zhang, W. Ou, C. Tian, X. Chen, et al., Myocyte enhancer factor 2A delays vascular endothelial cell senescence by activating the PI3K/p-Akt/SIRT1 pathway, Aging (Albany NY) 11 (11) (2019) 3768–3784.
[48] M. Zhou, P. Ren, Y. Zhang, S. Li, M. Li, P. Li, J. Shang, W. Liu, H. Liu, Shen-yuan-dan capsule attenuates atherosclerosis and foam cell formation by enhancing autophagy and inhibiting the PI3K/Akt/mTORC1 signaling pathway, Front. Pharmacol. 10 (2019) 603.
[49] C. Liu, G. Chen, Y. Chen, Y. Dang, G. Nie, D. Wu, J. Li, Z. Chen, H. Yang, D. He, et al., Danlou tablets inhibit atherosclerosis in apolipoprotein E-deficient mice by inducing macrophage autophagy: the role of the PI3K-Akt-mTOR pathway, Front. Pharmacol. 12 (2021) 724670.